



Published in final edited form as:

*Science*. 2010 July 30; 329(5991): 568–571. doi:10.1126/science.1189992.

## Identification of a cell-of-origin for human prostate cancer

**Andrew S. Goldstein**<sup>1</sup>, **Jiaoti Huang**<sup>2,3,8</sup>, **Changyong Guo**<sup>2,4</sup>, **Isla P. Garraway**<sup>2,4</sup>, and **Owen N. Witte**<sup>1,5,6,7,8</sup>

<sup>1</sup>Molecular Biology Institute, University of California, Los Angeles, CA 90095

<sup>2</sup>Jonsson Comprehensive Cancer Center, University of California, Los Angeles, CA 90095

<sup>3</sup>Department of Pathology and Laboratory Medicine, University of California, Los Angeles, CA 90095

<sup>4</sup>Department of Urology, University of California, Los Angeles, CA 90095

<sup>5</sup>Department of Microbiology, Immunology and Molecular Genetics, University of California, Los Angeles, CA 90095

<sup>6</sup>Department of Molecular and Medical Pharmacology, University of California, Los Angeles, CA 90095

<sup>7</sup>Howard Hughes Medical Institute, David Geffen School of Medicine, University of California, Los Angeles, CA 90095

<sup>8</sup>Eli and Edythe Broad Center of Regenerative Medicine and Stem Cell Research, University of California, Los Angeles, CA 90095

### Abstract

Prostate cancer induced in primary human prostate basal cells recapitulates disease initiation and progression in immunodeficient mice.

---

Luminal cells are believed to be the cells-of-origin for human prostate cancer because the disease is characterized by luminal cell expansion and absence of basal cells. Yet functional studies addressing the origin of human prostate cancer have not previously been reported due to a lack of relevant *in vivo* human models. Here we show that basal cells, from primary benign human prostate tissue, can initiate prostate cancer in immunodeficient mice. The cooperative effects of AKT, ERG, and androgen receptor (AR) in basal cells recapitulated the histological and molecular features of human prostate cancer with loss of basal cells and expansion of luminal cells expressing prostate-specific antigen (PSA) and alpha-methylacyl-CoA racemase (AMACR). Our results demonstrate that histological characterization of cancers does not necessarily correlate with the cellular origins of the disease.

Prostate cancer research has been hindered by an absence of model systems in which the disease is initiated from primary human prostate epithelial cells, precluding investigation of transforming alterations and cells-of-origin. Commonly used human prostate cancer cell lines and xenografts were derived from metastatic lesions. Murine prostate cancer models prohibit testing of species-specific therapies such as monoclonal antibodies against human proteins (1). An ideal model system would be human cell-derived and present as a multi-focal disease to accurately represent the heterogeneity of prostate malignancy (2). The

system should allow one to investigate the role that specific genetic alterations and paracrine signals play in disease initiation and progression. Finally, the model system should be highly malleable, allowing for comparisons of lesions derived from different cell populations or driven by different genetic alterations. We create such a system by directly transforming naïve adult human prostate epithelium with genetic alterations that are commonly found in human prostate cancer. Activation of the PI3K pathway, typically via loss of PTEN (3), and increased expression of the ETS family transcription factor ERG through chromosomal translocation (4) occur frequently together in human prostate cancer and cooperate to promote disease progression in mice (5–7). AR is commonly upregulated in human prostate cancer and the androgen signaling axis is implicated in late stage disease (8).

Luminal cells are generally accepted as the cells-of-origin for human prostate cancer (9,10) because pathologists diagnose the disease based on the absence of basal cell markers (11). Evidence from the mouse implicates both luminal cells (12–14) and basal cells (15–17) in prostate cancer initiation. While murine cancer cell-of-origin studies typically involve transgenic mice with oncogene expression or Cre-mediated deletion of tumor suppressors driven by cell-type specific promoters (18), parallel studies in the human system require both a method to reliably separate sub-populations of primary cells and an *in vivo* transformation model.

In addition to rare neuroendocrine cells and reported intermediate phenotypes, the three main epithelial cell populations described in the human prostate are K5 (Keratin 5)+ K14+ K8/18<sup>lo</sup> basal cells, K5+ K14– K8/18<sup>lo</sup> basal cells, and K5– K14– K8/18<sup>hi</sup> luminal cells (19). No commonly accepted strategy exists to isolate such populations from dissociated human prostate tissue. We have previously demonstrated expression of CD49f (integrin alpha 6) and Trop2 (TACSTD2) in human prostate tissue by immunohistochemical staining and flow cytometry, where these two antigens distinguish four separate populations (20,21). To determine the cellular identities of each population, we performed intracellular flow cytometry for basal (K14) and luminal (K18) keratins on primary human prostate cells in addition to western blot and quantitative PCR (qRT-PCR) analyses on fractions isolated by fluorescence-activated cell sorting (FACS). The CD49f<sup>lo</sup>Trop2<sup>hi</sup> fraction expresses high levels of the luminal keratins K8 and K18, low or negative levels of basal keratins K5 and K14, and high expression of AR and several androgen-regulated genes such as PSA, Nkx3-1 and TMPRSS2 (Fig. 1A–C, fig S1). The CD49f<sup>hi</sup>Trop2<sup>hi</sup> fraction expresses high levels of K5 and the basal transcription factor p63, and two discrete peaks for K14 by intracellular flow cytometry, presumably containing both K14+ and K14– basal cells (Fig. 1A–C, fig S1). CD49f<sup>hi</sup>Trop2<sup>hi</sup> cells express intermediate levels of the luminal-type keratins (Fig. 1A), confirming previous reports that basal cells express low but detectable levels of K8/18 (19). CD117 (kit) expression is not enriched in either epithelial fraction (fig S1). The results from three different approaches confirm that we can reproducibly enrich for the isolation of basal and luminal epithelial cells from primary human prostate tissue. The remaining cells are negative for both epithelial keratins and gene expression analysis indicates enrichment for CD31+ von Willebrand factor (VWF)+ endothelial cells (CD49f<sup>hi</sup>Trop2<sup>–</sup>) and CD90+ Vimentin+ stromal cells (CD49f<sup>lo</sup>Trop2<sup>–</sup>) (Fig. 1A–C, fig S1).

Classic human epithelial transformation studies involve an initial selection process via immortalization through manipulation with genetic influences like the SV40 T-antigen and/or the catalytic subunit of telomerase in addition to the selected oncogenes (22). We wanted to avoid culture selection by directly transforming primary cells prior to transplantation, so we looked to a recent report by Morrison and colleagues to gain insight into *in vivo* conditions. Quintana *et al.* reported that the number of primary human melanoma cells capable of tumor formation could be vastly improved by transplanting primary cells subcutaneously with Matrigel into NOD-SCID-IL2R $\gamma$ <sup>null</sup> (NSG) mice (23). Adapting this

strategy, we transduced primary human prostate cells with lentivirus, combined these cells with murine Urogenital Sinus Mesenchyme (UGSM) cells in Matrigel and injected subcutaneously into NSG mice. Starting materials were obtained from patients undergoing radical prostatectomy surgeries and benign tissues were carefully separated from cancer by an experienced Urologic Pathologist. Benign starting materials were negative for expression of human prostate malignancy markers and displayed no features of histologic transformation (fig. S2). Transplantation of cells without genetic modification never resulted in PIN or cancer, demonstrating an absence of malignant cells in starting materials.

We transduced  $10^5$  primary human prostate basal or luminal cells with a control lentivirus carrying the fluorescent marker RFP and found that both cell types were capable of lentiviral transduction (fig. S3). We next combined freshly-sorted cells with UGSM in Matrigel and transplanted into NSG mice. Although we were concerned that one cell type might preferentially undergo apoptosis in response to sorting, injection or residence in the subcutaneous space, we found that both cell types survived at relatively equal rates (fig. S4). When grafts were harvested after 8–16 weeks in vivo, outgrowths were only observed from basal cells (Fig. 1D). Luminal-derived grafts lacked epithelial structures and mimicked transplantation of UGSM cells alone (Fig. 1D). Basal-derived prostatic tubules exhibited a remarkable similarity to the native architecture of the gland, demonstrated by an outer K5+ p63+ basal cell layer and one or multiple K8+ AR+ luminal layers (Fig. 1E). As few as 5,000 basal cells were sufficient to generate ducts with distinct basal and luminal layers (table S1). Dissociated cells from grafts recapitulated the original four populations by flow cytometry discerned by expression of Trop2 and CD49f (Fig. 1F). Staining for a human-specific Trop2 antibody confirmed the development of human prostatic tissue (fig. S5). Results were reproducible for four independent patient samples and showed little variation between replicate grafts.

We next introduced a lentivirus carrying both activated (myristoylated) AKT and ERG (7) into primary basal and luminal cells (Fig. 2A). After 8–16 weeks in vivo, we observed the development of abnormal structures expressing AKT, nuclear ERG and the fluorescently linked marker RFP (Fig. 2B, 2D) from primary basal cells but not luminal cells (Fig. 2B). Structures lacking RFP expression, indicating an absence of lentiviral infection, were benign, demonstrating the requirement for expression of oncogenes to initiate a malignant phenotype. We observed an expansion of AR+ luminal-like cells with retention of the p63+ basal layer in basal cell-derived lesions (Fig. 2C). In many areas, cells were positive for both PSA and AMACR (Fig. 2C), a marker of both high grade PIN and prostate cancer (24). Based on the presence of morphologically malignant AR+/PSA+ luminal cells surrounded by p63+ basal cells, basal cell-derived lesions fulfill the histological criteria for the diagnosis of high grade PIN, the precursor lesion to invasive prostate cancer (25).

We evaluated if additional genetic alterations could be used to recapitulate human prostate cancer. Primary cells were transduced with the RFP-marked lentivirus carrying AKT and ERG and a GFP-marked lentivirus carrying AR (26) (Fig. 3A). Combination of AKT, ERG and AR resulted in the development of adenocarcinoma from basal cells (Fig. 3B) but not luminal cells. While some basal cell-derived structures retained expression of p63 and resembled PIN (fig. S6), many glands had lost the basal layer (Fig. 3B, fig. S6), a defining histological feature used by pathologists for the diagnosis of human prostate cancer (11). Cancerous glands expressed PSA (Fig. 3B, fig S7), AR and AMACR (Fig. 3B) in patterns indistinguishable from patient samples of clinical prostate cancer (Fig. 3C). At high power, cells from cancer lesions exhibited hyperchromatic nuclei with visible nucleoli (Fig. 3B–C, H&E insets). Clinical prostate cancer presents as a multifocal disease with considerable heterogeneity of disease grade (2). Within the same grafts, we observed lesions that correspond to benign structures (AR+/PSA+/p63+/AMACR–), PIN (AR+/PSA+/p63+/

AMACR+) and cancer (AR+/PSA+/p63-/AMACR+), recapitulating the mixed histology found in cancer patients (fig. S6).

Cells within the basal fraction can regenerate benign prostate tissue in immunodeficient mice. Introduction of oncogenic alterations in the target cells can induce a disease that mimics human prostate cancer, establishing basal cells as one cell-of-origin for prostate cancer. Our results support studies in the mouse demonstrating that histological characterization of cancers in the absence of functional studies can be misleading for determining cells-of-origin (27–30). As the human prostate epithelial hierarchy is further delineated, additional cell-types may be identified with cancer-initiating properties.

Even though basal cells express low levels of AR, they share the property of androgen-independence (31) with late stage castration-resistant prostate cancer cells (8), suggesting that pathways involved in basal cell function and self-renewal may play a role in tumor cell survival and disease recurrence after androgen withdrawal. Therefore, further interrogation of target cells may provide insight into treatments for castration-resistant prostate cancer.

## Supplementary Material

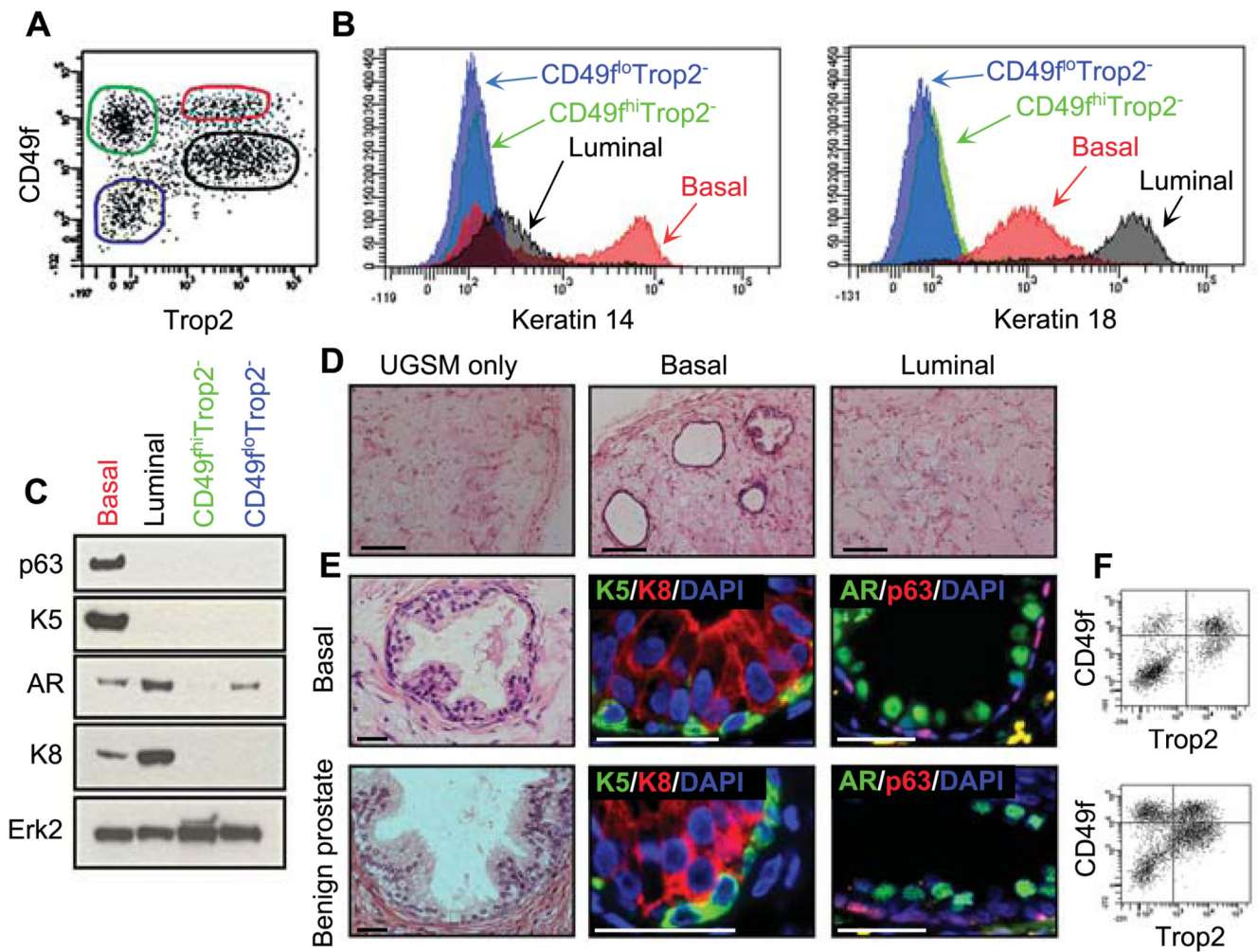
Refer to Web version on PubMed Central for supplementary material.

## References

1. Pienta KJ, et al. *Prostate* 2008 May 1;68:629. [PubMed: 18213636]
2. Ruijter ET, van de Kaa CA, Schalken JA, Debruyne FM, Ruiters DJ. *J Pathol* 1996 Nov;180:295. [PubMed: 8958808]
3. Yoshimoto M, et al. *Cancer Genet Cytogenet* 2006 Sep;169:128. [PubMed: 16938570]
4. Tomlins SA, et al. *Science* 2005 Oct 28;310:644. [PubMed: 16254181]
5. Carver BS, et al. *Nat Genet* 2009 May;41:619. [PubMed: 19396168]
6. King JC, et al. *Nat Genet* 2009 May;41:524. [PubMed: 19396167]
7. Zong Y, et al. *Proc Natl Acad Sci U S A* 2009 Jul 28;106:12465. [PubMed: 19592505]
8. Chen CD, et al. *Nat Med* 2004 Jan;10:33. [PubMed: 14702632]
9. Okada H, et al. *Virchows Arch A Pathol Anat Histopathol* 1992;421:157. [PubMed: 1381129]
10. Parsons JK, Gage WR, Nelson WG, De Marzo AM. *Urology* 2001 Oct;58:619. [PubMed: 11597556]
11. Wojno KJ, Epstein JI. *Am J Surg Pathol* 1995 Mar;19:251. [PubMed: 7532918]
12. Ma X, et al. *Cancer Res* 2005 Jul 1;65:5730. [PubMed: 15994948]
13. Wang X, et al. *Nature* 2009 Sep 24;461:495. [PubMed: 19741607]
14. Iwata T, et al. *PLoS One* 5:e9427. [PubMed: 20195545]
15. Lawson DA, et al. *Proc Natl Acad Sci U S A* Feb 9;107:2610. [PubMed: 20133806]
16. Mulholland DJ, et al. *Cancer Res* 2009 Nov 15;69:8555. [PubMed: 19887604]
17. Wang S, et al. *Proc Natl Acad Sci U S A* 2006 Jan 31;103:1480. [PubMed: 16432235]
18. Barker N, et al. *Nature* 2009 Jan 29;457:608. [PubMed: 19092804]
19. Verhagen AP, et al. *Cancer Res* 1992 Nov 15;52:6182. [PubMed: 1384957]
20. Goldstein AS, et al. *Proc Natl Acad Sci U S A* 2008 Dec 30;105:20882. [PubMed: 19088204]
21. Garraway IP, et al. *Prostate* Apr 1;70:491. [PubMed: 19938015]
22. Hahn WC, et al. *Nature* 1999 Jul 29;400:464. [PubMed: 10440377]
23. Quintana E, et al. *Nature* 2008 Dec 4;456:593. [PubMed: 19052619]
24. Wu CL, et al. *Hum Pathol* 2004 Aug;35:1008. [PubMed: 15297968]
25. McNeal JE, Bostwick DG. *Hum Pathol* 1986 Jan;17:64. [PubMed: 3943853]
26. Xin L, et al. *Proc Natl Acad Sci U S A* 2006 May 16;103:7789. [PubMed: 16682621]

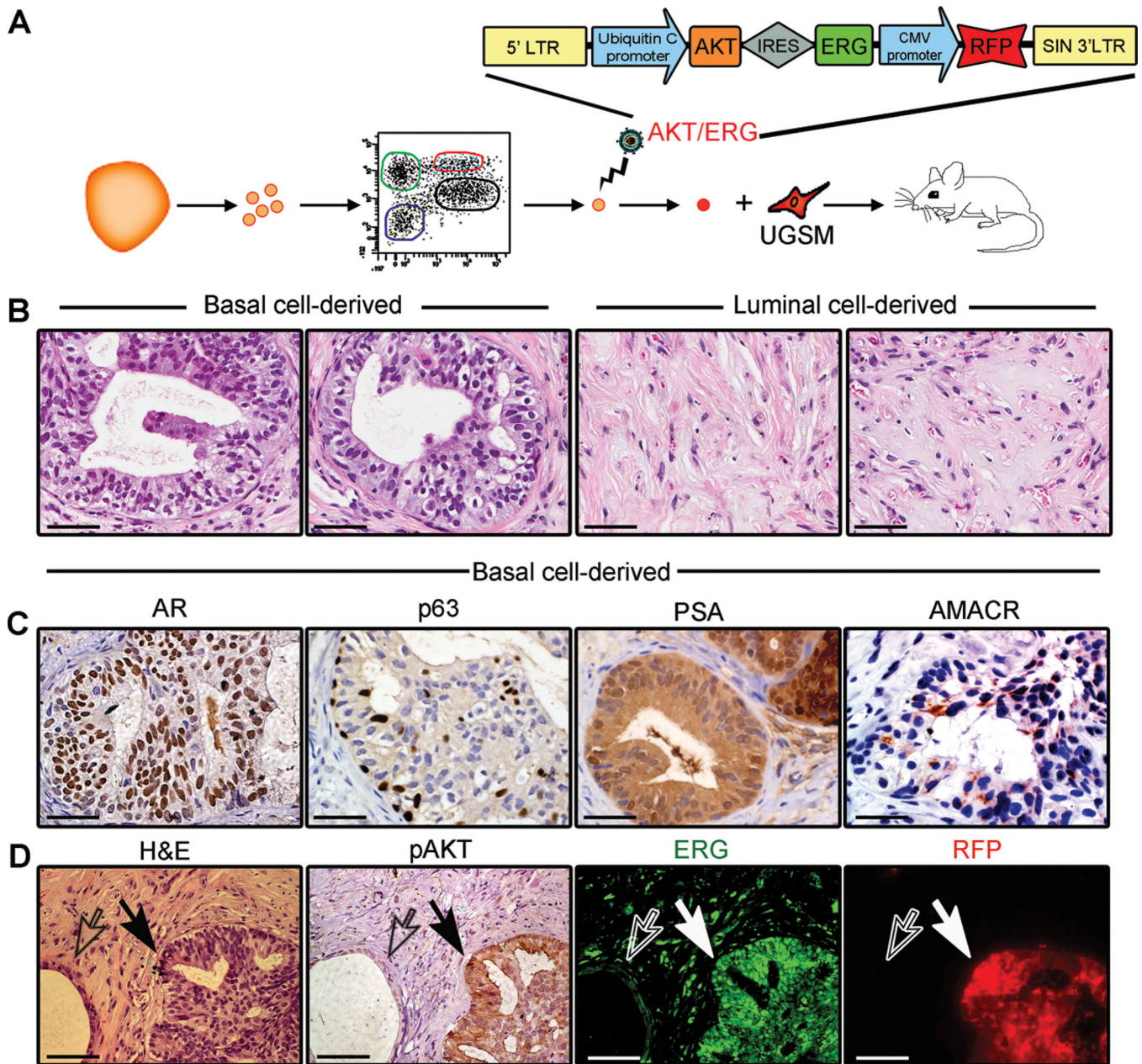
27. Youssef KK, et al. *Nat Cell Biol.* Feb 14;
28. Passegue E, Wagner EF, Weissman IL. *Cell* 2004 Oct 29;119:431. [PubMed: 15507213]
29. So CW, et al. *Cancer Cell* 2003 Feb;3:161. [PubMed: 12620410]
30. Cozzio A, et al. *Genes Dev* 2003 Dec 15;17:3029. [PubMed: 14701873]
31. English HF, Santen RJ, Isaacs JT. *Prostate* 1987;11:229. [PubMed: 3684783]
32. We thank Barbara Anderson for manuscript preparation, Donghui Cheng for cell sorting, Yang Zong for vectors, Hong Zhang for tissue preparation, and Akanksha Chhabra, Ben Van Handel, David Mulholland, Camille Soroudi and Tanya Stoyanova for discussion and technical help. A.S.G. is supported by an institutional Ruth L. Kirschstein National Research Service Award GM07185. J.H. is supported by the American Cancer Society, the DOD Prostate Cancer Research Program, and the UCLA SPORE in Prostate Cancer (Principal Investigator: Rob Reiter). I.P.G is supported by the DOD and the Jean Perkins Foundation. O.N.W. is an Investigator of the Howard Hughes Medical Institute. J.H., I.P.G. and O.N.W. are supported by a Challenge Award from the Prostate Cancer Foundation.





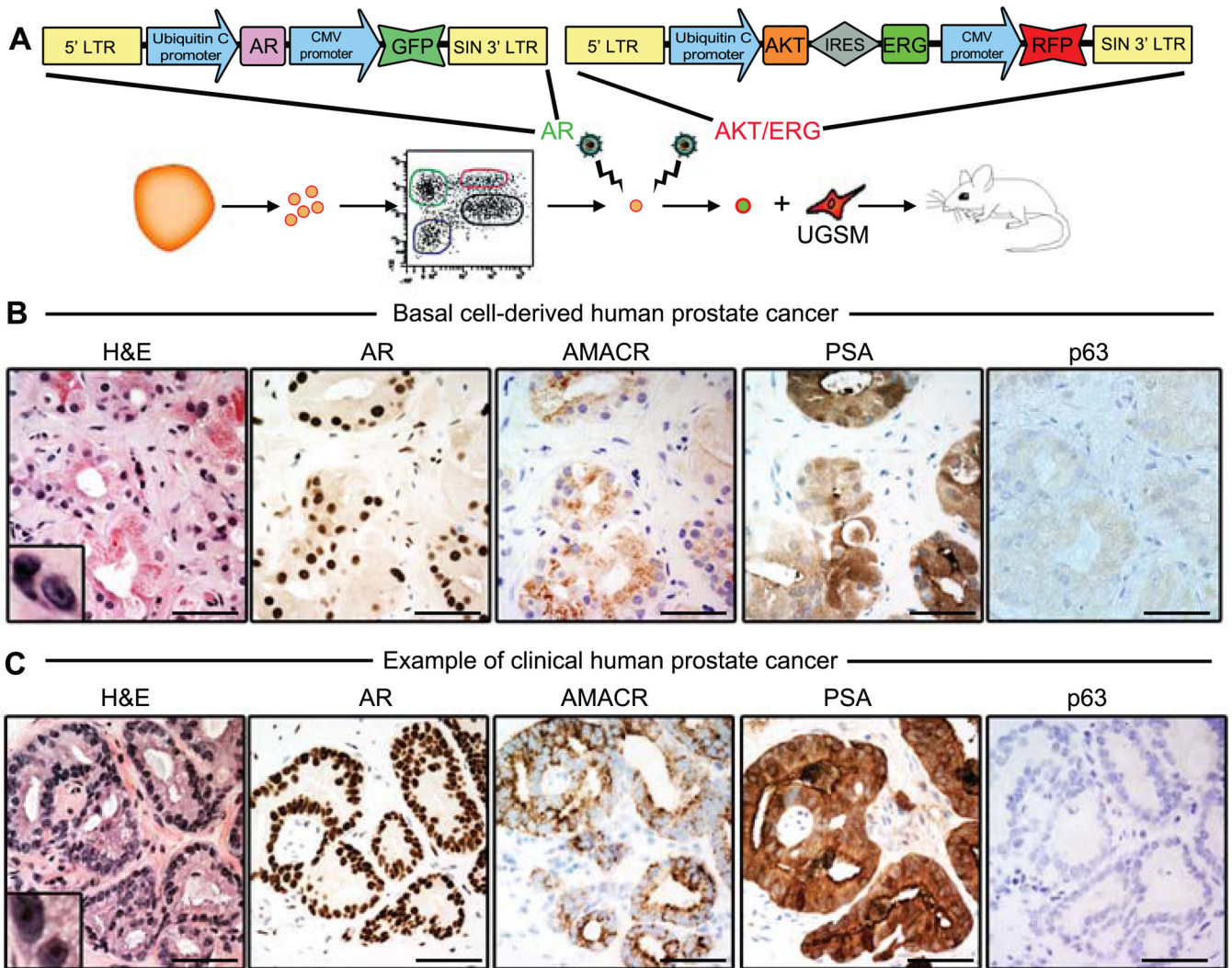
**Fig. 1.**

Purification of epithelial cell fractions from primary prostate tissue. (A) FACS plots show the distribution of dissociated primary prostate cells based on expression of CD49f and Trop2 and gates drawn to distinguish four populations. (B) Expression of Keratin 14 (K14) and Keratin 18 (K18) for each of the four populations indicated in A. (C) Immunoblots of lysates from each subpopulation analyzed for expression of basal proteins Keratin 5 (K5) and p63, and luminal proteins Keratin 8 (K8) and androgen receptor (AR). Erk2 is included as a loading control. (D) Haematoxylin and eosin (H&E) stained sections of outgrowths generated from dissociated cells transplanted subcutaneously into NSG mice. Scale bars, 200  $\mu$ m. (E) Tissue generated from human prostate basal cells (top row) resembles benign human prostate tissue (bottom row). H&E shows tubule structure. High power images of immunostained prostatic tubules demonstrate presence of distinct basal and luminal layers. Yellow spots are negative for DAPI and indicate auto-fluorescent spots rather than nuclei. Scale bars, 40  $\mu$ m. (F) FACS plots show presence of four populations with regards to CD49f and Trop2 staining on dissociated cells from basal-derived outgrowths or benign human prostate tissue.



**Fig. 2.** A model of PIN initiated in primary basal cells. (A) Schematic of cell sorting, lentiviral infection (with bicistronic vector encoding activated/myristoylated AKT, ERG and the fluorescent marker RFP) and transplantation to induce initiation of PIN. (B) Images of H&E stained sections of grafts derived from transduced basal and luminal cells. Scale bars, 50  $\mu$ m. (C) Immunohistochemistry of basal cell-derived lesions demonstrates prominent nuclear expression of AR with retention of p63+ cells, and cytoplasmic staining for PSA and AMACR within PIN lesions. Scale bars, 50  $\mu$ m. (D) Serial sections of basal cell-derived PIN (closed arrow) next to a benign tubule (open arrow) that was not infected with lentivirus. High levels of expression of RFP (red), membrane-bound phospho-AKT (brown), and nuclear ERG (green) in PIN (closed arrow) but not in the neighboring un-infected benign tubule (open arrow). Scale bars, 100  $\mu$ m.



**Fig. 3.**

A model of prostate cancer initiated in primary basal cells. (A) Schematic of cell sorting, double lentiviral infection (with GFP-encoding AR vector and bicistronic AKT/ERG vector) and transplantation to induce initiation of prostate cancer. (B–C) High-power images show similar staining patterns between basal cell-derived human prostate cancer (B) and clinical human prostate cancer (C). H&E insets demonstrate hyperchromatic nuclei with visible nucleoli at high magnification. Cancer lesions are positive for AR, AMACR and PSA and do not express the basal cell marker p63. Scale bars, 50  $\mu$ m. Low power images provided in fig. S6 demonstrate heterogeneity of disease grade in both clinical human prostate cancer and basal cell-derived human prostate cancer with co-existence of benign, PIN and cancer structures.